

---

This item was submitted to [Loughborough's Research Repository](#) by the author.  
Items in Figshare are protected by copyright, with all rights reserved, unless otherwise indicated.

## High-performance electrochemical CO<sub>2</sub> reduction cells based on non-noble metal catalysts

PLEASE CITE THE PUBLISHED VERSION

<https://doi.org/10.1021/acsenergylett.8b01681>

PUBLISHER

© American Chemical Society

VERSION

AM (Accepted Manuscript)

PUBLISHER STATEMENT

This document is the Accepted Manuscript version of a Published Work that appeared in final form in ACS Energy Letters, copyright © American Chemical Society after peer review and technical editing by the publisher. To access the final edited and published work see <https://pubs.acs.org/doi/10.1021/acsenergylett.8b01681>.

LICENCE

CC BY-NC-ND 4.0

REPOSITORY RECORD

Lu, Xu, Yueshen Wu, Xiaolei Yuan, Ling Huang, Zishan Wu, Jin Xuan, Yifei Wang, and Hailiang Wang. 2018. "High-performance Electrochemical CO<sub>2</sub> Reduction Cells Based on Non-noble Metal Catalysts". figshare. <https://hdl.handle.net/2134/36188>.

## High Performance Electrochemical CO<sub>2</sub> Reduction Cells Based on Non-Noble Metal Catalysts

Xu Lu<sup>1,2</sup>, Yueshen Wu<sup>1,2</sup>, Xiaolei Yuan<sup>1,2,3</sup>, Ling Huang<sup>1,2,4</sup>, Zishan Wu<sup>1,2</sup>, Jin Xuan<sup>5</sup>, Yifei Wang<sup>6</sup>,  
Hailiang Wang<sup>1,2\*</sup>

<sup>1</sup> Department of Chemistry, Yale University, New Haven, Connecticut 06520, United States

<sup>2</sup> Energy Sciences Institute, Yale University, West Haven, Connecticut 06516, United States

<sup>3</sup> Institute of Functional Nano and Soft Materials (FUNSOM), Jiangsu Key Laboratory for Carbon-Based Functional Materials and Devices, Soochow University, Suzhou, China

<sup>4</sup> Department of Advanced Energy Materials, Sichuan University, Chengdu, China

<sup>5</sup> Department of Chemical Engineering, Loughborough University, Loughborough, United Kingdom

<sup>6</sup> Department of Mechanical Engineering, University of Hong Kong, Hong Kong, China

Xu Lu and Yueshen Wu contributed equally to this work

\* Corresponding author: Prof. Hailiang Wang (E-mail: hailiang.wang@yale.edu)

### Abstract

The promise and challenge of electrochemical mitigation of carbon dioxide calls for innovations at the catalyst material level as well as at the reactor level. In this work, enabled by our high-performance and earth-abundant electrocatalyst materials for carbon dioxide reduction reactions, we developed alkaline micro-flow electrolytic cells for energy-efficient, selective, fast and durable carbon dioxide conversion to carbon monoxide and formate. With a cobalt phthalocyanine-based cathode catalyst, the carbon monoxide-selective cell starts to operate at a 0.26 V overpotential and reaches a Faradaic efficiency of 94% and a partial current density of 31 mA/cm<sup>2</sup> at a 0.56 V overpotential. With a tin dioxide-based cathode catalyst, the formate-selective cell starts to operate at a 0.76 V overpotential and reaches a Faradaic efficiency of 82% and a partial current density of 113 mA/cm<sup>2</sup> at a 1.36 V overpotential. In contrast to previous studies, we found that the overpotential reduction from using the alkaline electrolyte is mostly contributed by a pH gradient near the cathode surface.

### Introduction

Electrochemical conversion of CO<sub>2</sub> offers a promising solution to offset the greenhouse gas and ocean acidification issues. This process is particularly appealing when the transformation of concentrated carbon emissions into fuels or chemical feedstocks is driven by excess electricity generated from renewable sources<sup>1-3</sup>. Among various CO<sub>2</sub> reduction reaction (CO<sub>2</sub>RR) options, Formate (HCOO<sup>-</sup>) synthesis is one of the most viable technology pathways as the cost could be leveled to \$0.46/kg, below the commercial formic acid price threshold<sup>4</sup>. CO production, if coupled with the Fischer-Tropsch process, is also plausible with the potential to produce diesel fuel at the cost of \$4.4/gallon per gas equivalent<sup>1,4</sup>. More reduced products, such

as ethanol, are limited by a minimum cost of \$8.2/gallon per gas equivalent, lacking technoeconomic feasibility<sup>4</sup>. However, HCOO<sup>-</sup> synthesis and CO production are still hindered by inefficient kinetics. In this perspective, designing active, selective, durable and low-cost CO<sub>2</sub>RR catalysts is the key. Meanwhile, to push CO<sub>2</sub>RR toward a higher level of industrial relevance, it is important to improve the full-cell performance by developing reactors with enhanced mass transport and reduced internal resistance.

Extensive effort has been devoted to the search for efficient CO<sub>2</sub>RR catalyst materials. Some noble metals are both active and selective, such as Au for CO<sub>2</sub>-to-CO conversion<sup>5-7</sup> and Pd for HCOOH generation<sup>8,9</sup>. However, their high cost and low catalytic stability are less suitable for practical electrochemical reactors. Cu-based catalysts have displayed a wide product spectrum covering CO<sup>10</sup>, CH<sub>4</sub><sup>11,12</sup>, C<sub>2</sub>H<sub>4</sub><sup>13,14</sup>, HCOO<sup>-</sup><sup>15</sup> and multi-carbon species<sup>11,16</sup>. Yet, high selectivity and long-term stability are still not easy to achieve<sup>17</sup>. SnO<sub>x</sub> is able to reduce CO<sub>2</sub> to HCOO<sup>-</sup> with high Faradaic efficiency (FE) and good stability<sup>18</sup>, and it has been reported that its catalytic performance can be improved by hybridizing with a Cu<sup>19,20</sup> or Ag<sup>21</sup> component. For CO<sub>2</sub>-to-CO conversion, we have recently developed a hybrid material with molecularly-structured catalytic sites, namely cyano-substituted cobalt phthalocyanine molecules (CoPc-CN) anchored on carbon nanotubes (CNTs), which demonstrates high selectivity, large geometric current density and high turnover frequency at a relatively low overpotential<sup>22</sup>.

In the pursuit of electrochemical reactors for CO<sub>2</sub> reduction, the majority of reported studies has been based on two-compartment H-shape cells<sup>23,24</sup>. A cell voltage above 3 V is typically required to reach a moderate current density of 6 mA/cm<sup>2</sup><sup>23,24</sup>. Typical H cells are also subject to low maximum reaction rates limited by mass transport, due to the relatively large thickness of boundary layers<sup>25</sup>. Introducing a membrane electrode assembly was effective in reducing the distance between the two electrodes, but at the cost of either a high catalyst loading or a low product yield<sup>26,27</sup>. The effects of ionomers in MEA cells remain to be fully understood<sup>28</sup>. Adopting flow cells with gas diffusion electrodes (GDEs) was able to further improve the device performance<sup>29-33</sup>, and should also in theory be able to separate more clearly the effects of electrolyte composition on mass transport vs reaction kinetics in comparison to the H-cell design<sup>34-36</sup>, although researchers have not fully understood the three-phase interface. In particular, Kenis et al. achieved a current density of 135 mA/cm<sup>2</sup> and a FE<sub>CO</sub> of 95% at a cell voltage of 2.5 V in spite of the voltage loss caused by the relatively large inter-electrode distance, based on Ag nanoparticles as the cathode catalyst and a 1 M KOH aqueous solution as the electrolyte. This strategy<sup>29</sup> was also extended to other noble metal catalysts<sup>30-32</sup>. The onset cell voltage reduction from using the alkaline electrolyte was first explained by destabilization of the CO<sub>2</sub><sup>-</sup> intermediate by specific anions absorbed on Ag surface<sup>29</sup> and in a later study attributed to the non-proton-coupled rate-determining electron transfer step on Au surface<sup>33</sup>. The latter explanation would make sense if CO<sub>2</sub> does not react with KOH on the cathode and alter the pH near the catalyst surface, which remains to be verified by experimentally probing the local pH.

Here we report electrochemical flow cells equipped with catalysts based on earth-abundant elements that can perform selective and efficient CO<sub>2</sub> reduction to CO or HCOO<sup>-</sup>. With CoPc-CN/CNT as the cathode catalyst and CoO<sub>x</sub>/CNT as the anode catalyst, our cell starts to split CO<sub>2</sub> into CO and O<sub>2</sub> at a full-cell voltage of 1.6 V, corresponding to a nominal cell overpotential (*i.e.*  $\eta_{\text{cell}}$ ) of 0.26 V. The peak FE<sub>CO</sub> of 94% is reached at  $\eta_{\text{cell}} = 0.56$  V and a partial current density (*i.e.*  $j_{\text{CO}}$ ) of 31 mA/cm<sup>2</sup>.  $j_{\text{CO}}$  exceeds 80 mA/cm<sup>2</sup> at  $\eta_{\text{cell}} = 0.96$  V. With SnO<sub>2</sub>/CNT as the cathode catalyst, conversion of CO<sub>2</sub> and H<sub>2</sub>O to HCOO<sup>-</sup> and O<sub>2</sub> occurs at a full-cell voltage of 1.9 V, corresponding to a  $\eta_{\text{cell}}$  of 0.76 V. The FE<sub>HCOO<sup>-</sup></sub> reaches 82% at  $\eta_{\text{cell}} = 1.36$  V and  $j_{\text{HCOO<sup>- mA/cm<sup>2</sup>. The  $j_{\text{HCOO<sup>-</sup>}}$  approaches 200 mA/cm<sup>2</sup> at  $\eta_{\text{cell}} = 1.76$  V. Our devices represent the most efficient non-noble metal catalyst-based electrolytic cells that have been reported to date for reducing CO<sub>2</sub> to CO or HCOO<sup>-</sup>. Further analysis attributes the high electrochemical performance to our active, selective and durable CO<sub>2</sub>RR catalysts, to the low internal resistance and enhanced mass transport of the micro-flow cell, and importantly, to a pH gradient created by the neutralization of OH<sup>-</sup> by CO<sub>2</sub> near the cathode surface.</sup>$

## Results

The core component of our CO<sub>2</sub> electroreduction system (Fig. S1) is a micro-flow cell that facilitates two laminar electrolyte fluids (*i.e.* anolyte and catholyte) and a CO<sub>2</sub> gas stream to flow in parallel along micro-scale channels (Fig. 1). We note that gaseous products (CO or H<sub>2</sub>) could be mixed in either the CO<sub>2</sub> gas stream or the liquid catholyte, which was not explicitly discussed in the previous studies on similar cells. To ensure accurate product quantification, we invented a gas-tight collector, into which both the gas and electrolyte effluents were driven (Fig. S1). All the gaseous products could therefore be collected for online gas chromatograph sampling. The effectiveness of this design was vindicated by near-unity total FEs. The functionality of the micro-flow cell was first verified by using Au nanoparticles (Fig. S2) as the cathode catalyst for CO<sub>2</sub>RR, CoO<sub>x</sub>/CNT (Fig. S3) as the anode catalyst for the O<sub>2</sub> evolution reaction (OER), and a 0.5 M KHCO<sub>3</sub> aqueous solution as the electrolyte. The Au cathode demonstrated comparable electrocatalytic performance in the flow cell (Fig. S4) with that in a prevalent three-electrode H cell (Fig. S2) over a wide cathode potential range.

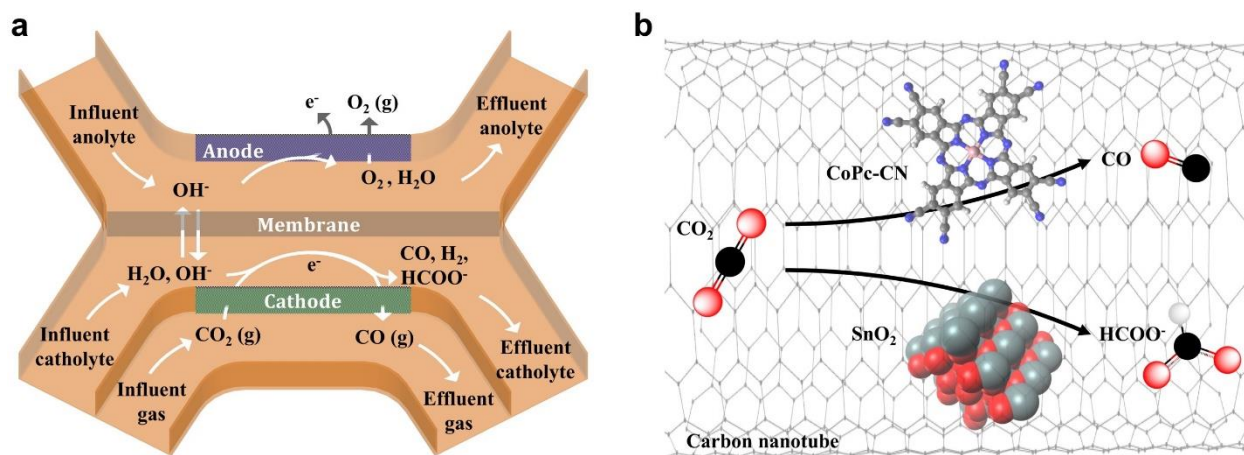


Figure 1. (a) Gas and liquid flows and electrochemical reactions in the flow cell; (b) CoPc-CN molecules and SnO<sub>2</sub> nanoparticles supported on CNTs as cathode electrocatalysts for CO<sub>2</sub> conversion to CO and HCOO<sup>-</sup>, respectively.

Our CO-producing cell employs CoPc-CN/CNT (Fig. S5) as the cathode catalyst and CoO<sub>x</sub>/CNT as the anode catalyst in a 1 M KOH aqueous electrolyte. Significant CO generation could be observed at a full-cell voltage as low as 1.6 V (Fig. 2a), which corresponds to a  $\eta_{\text{cell}}$  of 0.26 V and represents one of the lowest that have been reported for electrochemical CO<sub>2</sub> conversion to CO (Table S1). As the cell voltage was increased, CO production became more substantial. At a cell voltage of 1.9 V (*i.e.*  $\eta_{\text{cell}} = 0.56$  V), FE<sub>CO</sub> reached 94% with  $j_{\text{CO}} = 31$  mA/cm<sup>2</sup> (Fig. 2b). As the cell voltage was further elevated, CO selectivity decreased whereas  $j_{\text{CO}}$  continued to increase, reaching a maximum of 82 mA/cm<sup>2</sup> at a cell voltage of 2.3 V.  $j_{\text{H}_2}$  also increased with the cell voltage. At 2.7 V, H<sub>2</sub> became the dominant product with  $j_{\text{H}_2} = 168$  mA/cm<sup>2</sup> while FE<sub>CO</sub> dramatically dropped to 0.9% with  $j_{\text{CO}} = 1.5$  mA/cm<sup>2</sup>. The general dependence of product distribution on potential is in consistency with that measured for the same cathode catalyst in a three-electrode H cell (Fig. S5). A long-term operation was carried out for 10 h at a constant cell voltage of 2.0 V (*i.e.*  $\eta_{\text{cell}} = 0.66$  V), with the catholyte and anolyte being circulated separately. In spite of fluctuations due to gaseous bubble invasion and micro-flow disturbance,  $j_{\text{total}}$  stayed between 35 and 40 mA/cm<sup>2</sup> and FE<sub>CO</sub> was stable around 90% throughout the entire period (Fig. 2c). Stability at high performance as such has only been reported for an alkaline flow cell operating with a noble Au catalyst<sup>33</sup>.

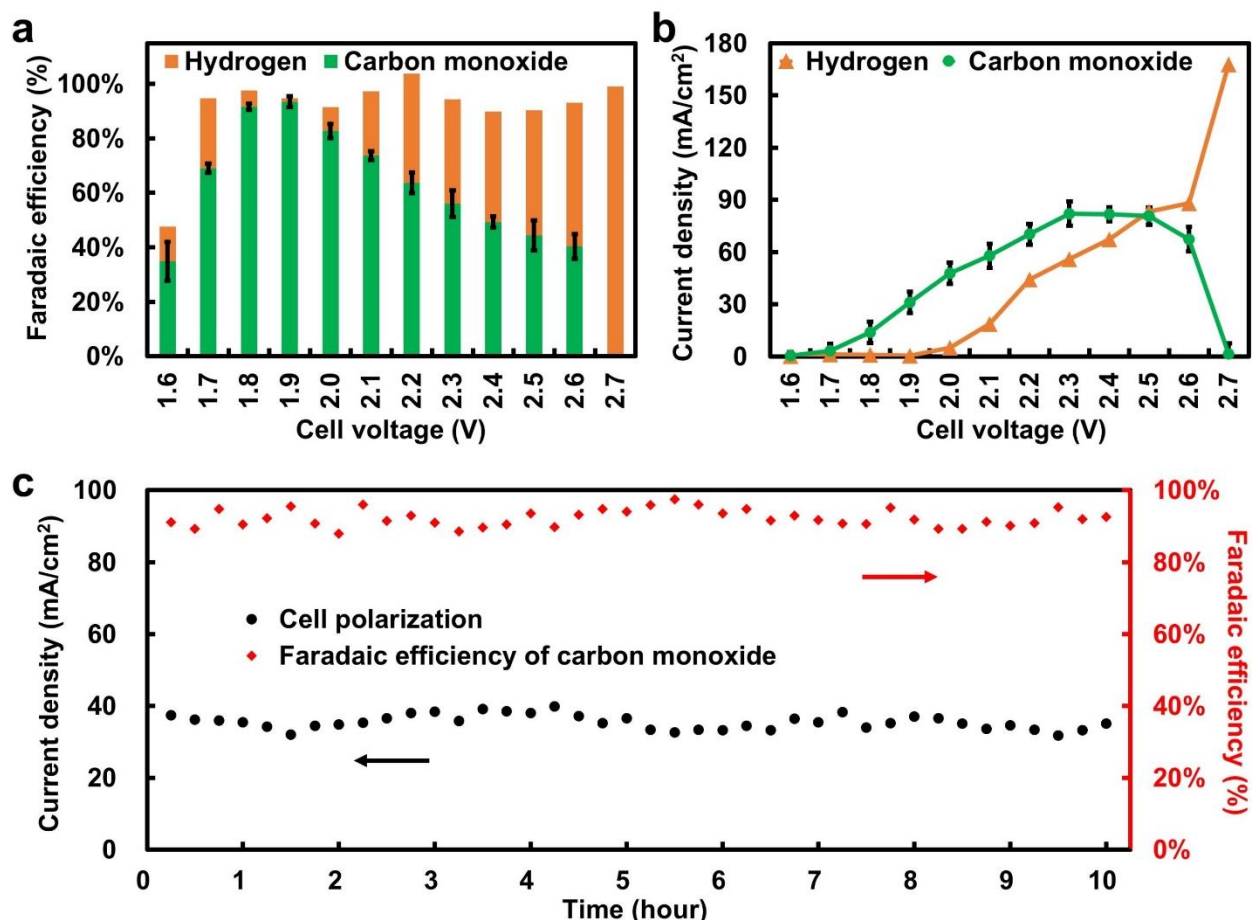


Figure 2. (a) Faradaic efficiencies and (b) partial current densities for CO and H<sub>2</sub> vs. the voltage of the electrolytic cell with CoPc-CN/CNT as the cathode catalyst, CoO<sub>x</sub>/CNT as the anode catalyst and 1 M KOH as the electrolyte; (c) Total current density and Faradaic efficiency for CO production during a 10 h operation at a constant cell voltage of 2.0 V. Error bars represent the standard deviations from multiple measurements.

We then steered the system to HCOO<sup>-</sup> production by switching the cathode catalyst to SnO<sub>2</sub>/CNT (Fig. S6). Significant HCOO<sup>-</sup> production could be detected at a cell voltage of 1.9 V (Fig. 3a), corresponding to a  $\eta_{\text{cell}}$  of 0.76 V.  $\text{FE}_{\text{HCOO}^-}$  increased with the applied cell voltage, reaching a maximum of 82% at a  $j_{\text{HCOO}^-}$  of 113 mA/cm<sup>2</sup> and a cell voltage of 2.5 V (*i.e.*  $\eta_{\text{cell}} = 1.36$  V). The high  $\text{FE}_{\text{HCOO}^-}$  of 80% was retained till the cell voltage was increased to 2.9 V, where  $j_{\text{HCOO}^-}$  approached 200 mA/cm<sup>2</sup> (Fig. 3b). This performance is close to industry-relevant levels<sup>37</sup> and outperforms some of the most efficient CO<sub>2</sub>-to-HCOO<sup>-</sup> electrolytic devices reported to date<sup>38-40</sup> (Table S1). Under the electrolyte circulation mode, the cell was operated at a constant cell voltage of 2.3 V (*i.e.*  $\eta_{\text{cell}} = 1.16$  V) for 35 h (Fig. 3c). The entire electrolysis yielded 0.7 M of HCOO<sup>-</sup> in the 12 mL electrolyte, with  $\text{FE}_{\text{HCOO}^-}$  between 60% and 70% and the total current density between 30 and 50 mA/cm<sup>2</sup>. The decay in selectivity and current density during the long-term electrolysis could be

attributed to the consumption of  $\text{OH}^-$  on the anode side and hence the gradual decrease in the pH of the anolyte. A lower pH on the anode side could worsen the OER kinetics and decrease the full-cell performance. While the pH of the catholyte is also expected to change, the local pH near the cathode catalyst surface is likely held stable by the chemical reaction between  $\text{CO}_2$  and  $\text{KOH}$ , which will be discussed below.

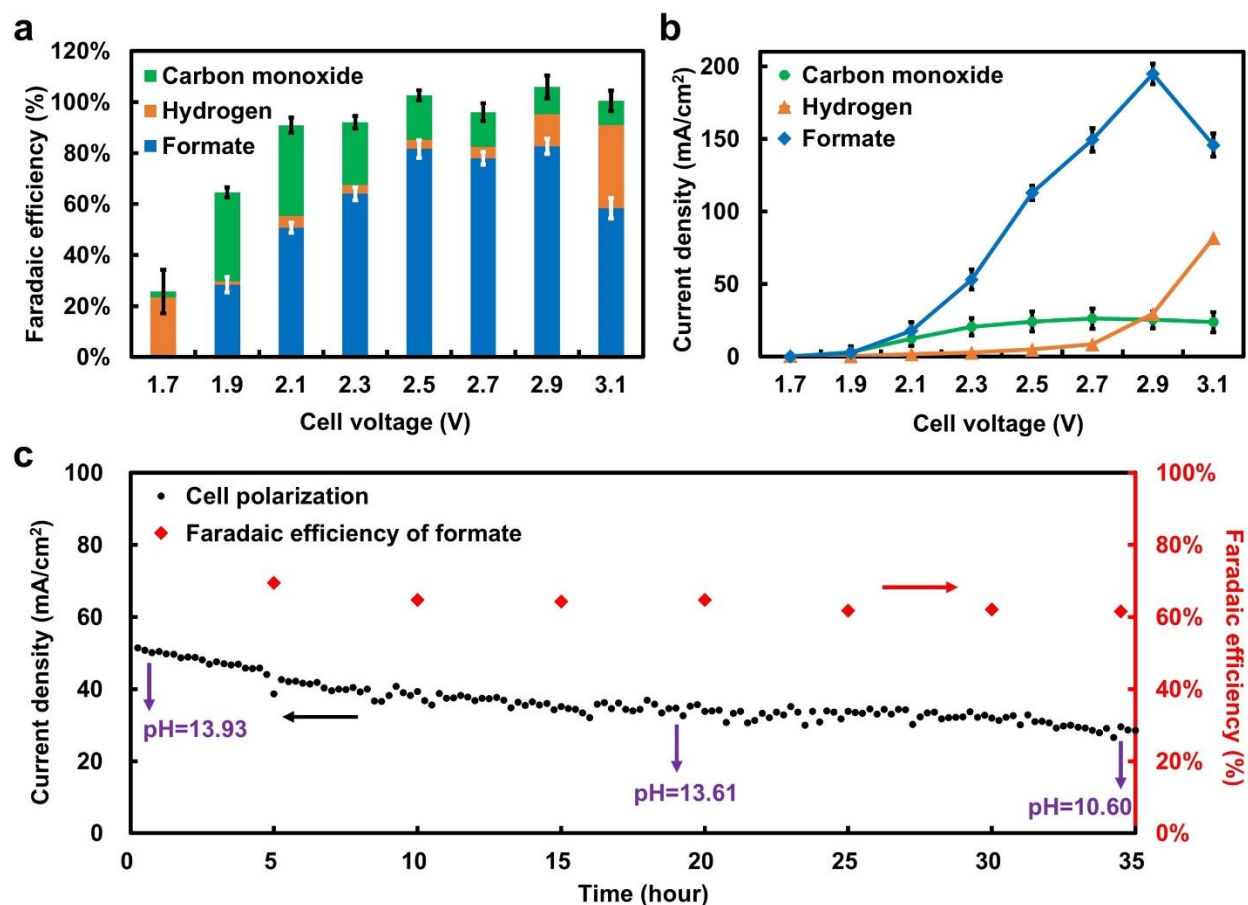


Figure 3. (a) Faradaic efficiencies and (b) partial current densities for  $\text{HCOO}^-$ ,  $\text{CO}$  and  $\text{H}_2$  vs. the voltage of the electrolytic cell with  $\text{SnO}_2/\text{CNT}$  as the cathode catalyst,  $\text{CoO}_x/\text{CNT}$  as the anode catalyst and 1 M  $\text{KOH}$  as the electrolyte; (c) Total current density and Faradaic efficiency for  $\text{HCOO}^-$  production during a 35 h operation at a constant cell voltage of 2.3 V; The catholyte was sampled for pH measurements at the 0<sup>th</sup>, 18<sup>th</sup> and 35<sup>th</sup> hour. Error bars represent the standard deviations from multiple measurements.

## Discussion

The high electrochemical performance is owing to both the catalysts and the cell design. The  $\text{CoPc-CN/CNT}$  and  $\text{SnO}_2/\text{CNT}$ , with high catalytic selectivity, activity and durability, ensure the efficient conversion of  $\text{CO}_2$  to  $\text{CO}$  and  $\text{HCOO}^-$ , respectively. The micro-flow cell architecture effectively minimizes the distance between the cathode and anode, and thus reduces the internal resistance (estimated to be 0.153

$\Omega/\text{cm}^2$ ). The GDE provides a three-phase interface for the electrochemical reactions to occur. The effective slip velocities at the GDE- $\text{CO}_2$  and GDE-electrolyte interfaces, in association with the parallel drift velocity profile near the electrode surface, reduce the diffusion boundary layer thickness and enhance the convective/diffusive mass transport. More essentially, the KOH electrolyte plays an indispensable role. In a control experiment using Au as the cathode catalyst and  $\text{CoO}_x/\text{CNT}$  as the anode catalyst, we found that the cell requires a 470 mV higher overpotential to reach a current density of  $20 \text{ mA}/\text{cm}^2$  when operating in a neutral  $0.5 \text{ M KHCO}_3$  electrolyte compared to that in the basic  $1 \text{ M KOH}$  electrolyte (Fig. 4, S4 and S7). The same situation occurs when using  $\text{CoPc-CN}/\text{CNT}$  (Fig. 2, 4 and S8) or  $\text{SnO}_2/\text{CNT}$  (Fig. 3, 4 and S9) as the cathode catalyst. While the voltage gain for the KOH cell can be partially explained by the situation that the OER is more efficient in alkaline than in neutral electrolyte<sup>41,42</sup>, there may be other important contributors to the observed performance improvement.

In another Au-based control experiment, we compared the KOH cell with a  $\text{KHCO}_3$  (catholyte)-KOH (anolyte) dual-electrolyte cell. These two cells exhibited very similar performances with respect to cell voltage, current density and  $\text{FE}_{\text{CO}}$  (Fig. 4, S10 and S11). It should be noted that the dual-electrolyte cell is benefited from the Nernst potential at the interface of the neutral catholyte and the basic anolyte. Therefore, the KOH cell has at least one more factor other than the OER kinetics that contributes to the overpotential reduction. It could be because of a more efficient  $\text{CO}_2\text{RR}$  in KOH than in  $\text{KHCO}_3$ , or a pH gradient similar to that in the dual-electrolyte cell.

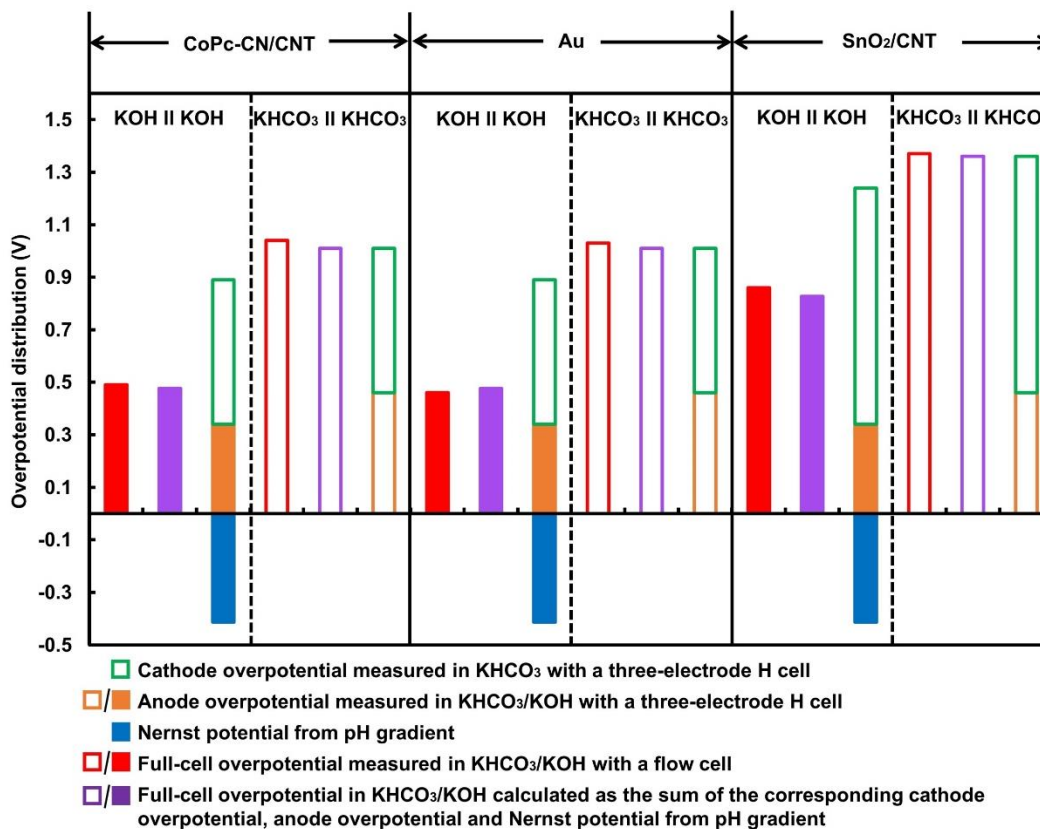


Figure 4. Contributions from cathode overpotential, anode overpotential and pH gradient to full-cell overpotential for micro-flow electrolytic cells operating at  $20 \text{ mA/cm}^2$  in alkaline or neutral electrolyte with three different cathode catalysts. Good match between the measured and calculated full-cell overpotentials supports our attribution of the overpotential reduction in alkaline electrolyte to the pH gradient and improvement of OER kinetics.

A previous study explained the cell performance improvement from using KOH electrolyte by assuming a proton-free rate-determining electron transfer step for the CO<sub>2</sub>-to-CO pathway on Au surface<sup>33</sup>, which implies that the CO<sub>2</sub> electroreduction kinetics is faster in more basic electrolyte. This rationale could be consistent with our results on the cells with Au or CoPc-CN/CNT as the cathode catalyst (an overpotential reduction of  $\sim 60 \text{ mV}$  per pH unit when switching from KOH to KHCO<sub>3</sub> electrolyte), for which the rate-determining step is likely to be non-proton-coupled electron transfer<sup>43,44</sup>. However, it cannot justify the performance of the SnO<sub>2</sub>/CNT-based cell, because CO<sub>2</sub> conversion to HCOO<sup>-</sup> is a two-electron/one-proton process, for which an assumption of a proton-free rate-determining electron transfer step would result a voltage gain of  $\sim 30 \text{ mV}$  per pH unit, contradicting our experimental observation. We propose that the existence of a pH gradient is a more suitable explanation to the universal performance improvement of all our KOH cells. Near the cathode surface, a near-neutral layer originates from the chemical reaction between

the penetrated CO<sub>2</sub> through the GDE and the KOH electrolyte. Deeper into the bulk where OH<sup>-</sup> dominates, the species balance shifts towards a more alkaline environment, creating a pH gradient and introducing a Nernst potential which reduces the overall cell voltage. In combination with the aforementioned pH-dependent OER overpotential which is a relatively minor effect, this can readily explain the overpotential dependence on electrolyte configuration for all our electrolytic cells based on three different cathode catalysts (Fig. 4). To verify that CO<sub>2</sub> indeed reacts with KOH at a considerable rate, we monitored the catholyte pH under the electrolyte circulation mode. While electrochemical CO<sub>2</sub>RR continues to consume protons, the OH<sup>-</sup> was nearly depleted after a 35 h operation (Fig. 3c).

## Conclusion

In conclusion, we have developed unprecedented electrochemical CO<sub>2</sub>RR cells based on non-noble metal catalysts for selective CO and HCOO<sup>-</sup> production at low voltages. Electrocatalytic conversion of CO<sub>2</sub> and H<sub>2</sub>O to CO or HCOO<sup>-</sup> and O<sub>2</sub> onsets at 0.26 and 0.76 V, respectively. High product selectivity, large current density and good durability are achieved at moderate overpotentials, rivaling the most up-to-date electrolytic CO<sub>2</sub>RR devices and approaching technological viability. The superior device performance is a combined result of good catalysts and cell design. This device is potentially suitable for a wide spectrum of catalysts, for instance Cu which can produce higher-order products such as ethylene and ethanol.

## Acknowledgement

This research is supported by the National Science Foundation (Grant CHE-1651717) and the Croucher Fellowship for Postdoctoral Research.

## Reference

- 1 Qiao, J., Liu, Y., Hong, F. & Zhang, J. A review of catalysts for the electroreduction of carbon dioxide to produce low-carbon fuels. *Chemical Society Reviews* **43**, 631-675 (2014).
- 2 Zhang, L., Zhao, Z. J. & Gong, J. Nanostructured materials for heterogeneous electrocatalytic CO<sub>2</sub> reduction and their related reaction mechanisms. *Angewandte Chemie International Edition* **56**, 11326-11353 (2017).
- 3 Seh, Z. W. *et al.* Combining theory and experiment in electrocatalysis: Insights into materials design. *Science* **355**, eaad4998 (2017).
- 4 Spurgeon, J. M. & Kumar, B. A comparative techno-economic analysis of pathways for commercial electrochemical CO<sub>2</sub> reduction to liquid products. *Energy & Environmental Science* **11**, 1536-1551 (2018).
- 5 Hori, Y., Kikuchi, K. & Suzuki, S. Production of CO and CH<sub>4</sub> in electrochemical reduction of CO<sub>2</sub> at

- metal electrodes in aqueous hydrogencarbonate solution. *Chemistry Letters* **14**, 1695-1698 (1985).
- 6 Fang, Y. & Flake, J. C. Electrochemical reduction of CO<sub>2</sub> at functionalized Au electrodes. *Journal of the American Chemical Society* **139**, 3399-3405 (2017).
  - 7 Zhao, S., Jin, R. & Jin, R. Opportunities and challenges in CO<sub>2</sub> reduction by gold and silver-based electrocatalysts: From bulk metals to nanoparticles and atomically precise nanoclusters. *ACS Energy Letters* **3**, 452–462 (2018).
  - 8 Min, X. & Kanan, M. W. Pd-catalyzed electrohydrogenation of carbon dioxide to formate: high mass activity at low overpotential and identification of the deactivation pathway. *Journal of the American Chemical Society* **137**, 4701-4708 (2015).
  - 9 Gao, D. *et al.* Switchable CO<sub>2</sub> electroreduction via engineering active phases of Pd nanoparticles. *Nano Research* **10**, 2181-2191 (2017).
  - 10 Cao, L. *et al.* Mechanistic insights for low-overpotential electroreduction of CO<sub>2</sub> to CO on copper nanowires. *ACS Catalysis* **7**, 8578-8587 (2017).
  - 11 Li, Y. *et al.* Structure-sensitive CO<sub>2</sub> electroreduction to hydrocarbons on ultrathin 5-fold twinned copper nanowires. *Nano letters* **17**, 1312-1317 (2017).
  - 12 Weng, Z. *et al.* Active sites of copper-complex catalytic materials for electrochemical carbon dioxide reduction. *Nature communications* **9**, 415 (2018).
  - 13 Reller, C. *et al.* Selective electroreduction of CO<sub>2</sub> toward ethylene on nano dendritic copper catalysts at high current density. *Advanced Energy Materials* **7** (2017).
  - 14 Mistry, H. *et al.* Highly selective plasma-activated copper catalysts for carbon dioxide reduction to ethylene. *Nature communications* **7**, 12123 (2016).
  - 15 Shinagawa, T., Larrazábal, G. O., Martín, A. J., Krumeich, F. & Perez Ramirez, J. Sulfur-modified copper catalysts for the electrochemical reduction of carbon dioxide to formate. *ACS Catalysis* **8**, 837-844 (2017).
  - 16 Weng, Z. *et al.* Electrochemical CO<sub>2</sub> reduction to hydrocarbons on a heterogeneous molecular Cu catalyst in aqueous solution. *Journal of the American Chemical Society* **138**, 8076-8079 (2016).
  - 17 Weng, Z. *et al.* Self-cleaning catalyst electrodes for stabilized CO<sub>2</sub> reduction to hydrocarbons. *Angewandte Chemie International Edition* **56**, 13135-13139 (2017).
  - 18 Zhang, S., Kang, P. & Meyer, T. J. Nanostructured tin catalysts for selective electrochemical reduction of carbon dioxide to formate. *Journal of the American Chemical Society* **136**, 1734-1737 (2014).
  - 19 Li, Q. *et al.* Tuning Sn-catalysis for electrochemical reduction of CO<sub>2</sub> to CO via the core/shell Cu/SnO<sub>2</sub> structure. *Journal of the American Chemical Society* **139**, 4290-4293 (2017).
  - 20 Huo, S. *et al.* Coupled metal/oxide catalysts with tunable product selectivity for electrocatalytic CO<sub>2</sub> reduction. *ACS applied materials & interfaces* **9**, 28519-28526 (2017).

- 21 Luc, W. *et al.* Ag-Sn bimetallic catalyst with a core-shell structure for CO<sub>2</sub> reduction. *Journal of the American Chemical Society* **139**, 1885-1893 (2017).
- 22 Zhang, X. *et al.* Highly selective and active CO<sub>2</sub> reduction electrocatalysts based on cobalt phthalocyanine/carbon nanotube hybrid structures. *Nature communications* **8**, 14675 (2017).
- 23 Morlanés, N., Takanabe, K. & Rodionov, V. Simultaneous reduction of CO<sub>2</sub> and splitting of H<sub>2</sub>O by a single immobilized cobalt phthalocyanine electrocatalyst. *ACS Catalysis* **6**, 3092-3095 (2016).
- 24 Tatin, A. *et al.* Efficient electrolyzer for CO<sub>2</sub> splitting in neutral water using earth-abundant materials. *Proceedings of the National Academy of Sciences* **113**, 5526-5529 (2016).
- 25 Clark, E. L. *et al.* Standards and protocols for data acquisition and reporting for studies of the electrochemical reduction of carbon dioxide. *ACS Catalysis* **8**, 6560-6570, doi:10.1021/acscatal.8b01340 (2018).
- 26 Narayanan, S., Haines, B., Soler, J. & Valdez, T. Electrochemical conversion of carbon dioxide to formate in alkaline polymer electrolyte membrane cells. *Journal of The Electrochemical Society* **158**, A167-A173 (2011).
- 27 Delacourt, C., Ridgway, P. L., Kerr, J. B. & Newman, J. Design of an electrochemical cell making syngas (CO+H<sub>2</sub>) from CO<sub>2</sub> and H<sub>2</sub>O reduction at room temperature. *Journal of The Electrochemical Society* **155**, B42-B49 (2008).
- 28 Xu, W. & Scott, K. The effects of ionomer content on PEM water electrolyser membrane electrode assembly performance. *International Journal of Hydrogen Energy* **35**, 12029-12037 (2010).
- 29 Verma, S., Lu, X., Ma, S., Masel, R. I. & Kenis, P. J. The effect of electrolyte composition on the electroreduction of CO<sub>2</sub> to CO on Ag based gas diffusion electrodes. *Physical Chemistry Chemical Physics* **18**, 7075-7084 (2016).
- 30 Ma, S., Liu, J., Sasaki, K., Lyth, S. M. & Kenis, P. J. Carbon foam decorated with silver nanoparticles for electrochemical CO<sub>2</sub> conversion. *Energy Technology* **5**, 861-863 (2017).
- 31 Hoang, T. T. *et al.* Nano porous copper-silver alloys by additive-controlled electro-deposition for the selective electroreduction of CO<sub>2</sub> to ethylene and ethanol. *Journal of the American Chemical Society* **140**, 5791-5797 (2018).
- 32 Seifitokaldani, A. *et al.* Hydronium-induced switching between CO<sub>2</sub> electroreduction pathways. *Journal of the American Chemical Society* **140**, 3833-3837 (2018).
- 33 Verma, S. *et al.* Insights into the low overpotential electroreduction of CO<sub>2</sub> to CO on a supported gold catalyst in an alkaline flow electrolyzer. *ACS Energy Letters* **3**, 193-198 (2017).
- 34 Resasco, J. *et al.* Promoter effects of alkali metal cations on the electrochemical reduction of carbon dioxide. *Journal of the American Chemical Society* **139**, 11277-11287 (2017).
- 35 Chen, L. D., Urushihara, M., Chan, K. & Nørskov, J. K. Electric field effects in electrochemical CO<sub>2</sub>

- reduction. *ACS Catalysis* **6**, 7133-7139 (2016).
- 36 Resasco, J., Lum, Y., Clark, E., Zeledon, J. Z. & Bell, A. T. Effects of Anion Identity and Concentration on Electrochemical Reduction of CO<sub>2</sub>. *ChemElectroChem* **5**, 1064-1072 (2018).
  - 37 Agarwal, A. S., Zhai, Y., Hill, D. & Sridhar, N. The electrochemical reduction of carbon dioxide to formate/formic acid: engineering and economic feasibility. *ChemSusChem* **4**, 1301-1310 (2011).
  - 38 Alvarez Guerra, M., Del Castillo, A. & Irabien, A. Continuous electrochemical reduction of carbon dioxide into formate using a tin cathode: Comparison with lead cathode. *Chemical Engineering Research and Design* **92**, 692-701 (2014).
  - 39 Jones, J. P., Prakash, G. & Olah, G. A. Electrochemical CO<sub>2</sub> reduction: recent advances and current trends. *Israel Journal of Chemistry* **54**, 1451-1466 (2014).
  - 40 Whipple, D. T., Finke, E. C. & Kenis, P. J. Microfluidic reactor for the electrochemical reduction of carbon dioxide: the effect of pH. *Electrochemical and Solid-State Letters* **13**, B109-B111 (2010).
  - 41 Gerken, J. B. *et al.* Electrochemical water oxidation with cobalt-based electrocatalysts from pH 0-14: the thermodynamic basis for catalyst structure, stability, and activity. *Journal of the American Chemical Society* **133**, 14431-14442 (2011).
  - 42 Zhao, Y. *et al.* Graphene-Co<sub>3</sub>O<sub>4</sub> nanocomposite as electrocatalyst with high performance for oxygen evolution reaction. *Scientific reports* **5**, 7629 (2015).
  - 43 Varela, A. S. *et al.* pH effects on the selectivity of the electrocatalytic CO<sub>2</sub> reduction on graphene-embedded Fe-N-C motifs: Bridging concepts between molecular homogeneous and solid-state heterogeneous catalysis. *ACS Energy Letters* **3**, 812-817 (2018).
  - 44 Chen, Y., Li, C. W. & Kanan, M. W. Aqueous CO<sub>2</sub> reduction at very low overpotential on oxide-derived Au nanoparticles. *Journal of the American Chemical Society* **134**, 19969-19972 (2012).